N_2O catalytic decomposition – from laboratory experiment to industry reactor

L. Obalová [a,b], K. Jirátová [c], K. Karásková [a], Ž. Chromčáková [a]

VŠB – Technical University of Ostrava, [a] Faculty of Metallurgy and Materials Engineering, [b] Centre for Environmental Technologies, 17. listopadu 15, 708 33 Ostrava, Czech Republic

[c] Institute of Chemical Process Fundamentals CAS v.v.i., Rozvojová 135, 165 02 Prague, Czech Republic

Abstract

Paper deals with design of pilot reactor for low temperature N_2O decomposition in off-gases from HNO_3 production. Pseudo-homogeneous one-dimensional model of an ideal plug flow reactor was used for modeling of N_2O decomposition in a laboratory fixed bed reactor filled with grains or pellets of a Co-Mn-Al mixed oxide catalyst. Increase in inlet pressure up to 0.6 MPa did not influence the effective diffusion coefficient, but improved the achieved N_2O conversion. Based on the laboratory data of N_2O decomposition over Co-Mn-Al mixed oxide pellets, catalyst bed of 3400 kg was estimated for target 90 % N_2O conversion (30 000 m^3 h^{-1} of exhaust gases from HNO_3 plant containing 0.1 molar% N_2O, 0.01 molar% NO, 0.01 molar% NO_2, 3 molar% H_2O, 5 molar% O_2) at 420 °C and 600 kPa inlet pressure.

Key words: N_2O, Catalytic decomposition, Fixed bed reactor, Effectiveness factor, Mixed oxide catalysts

1. Introduction

In the last years, the catalytic decomposition of N_2O as a method for abatement of N_2O emissions in waste gases attracted increasing attention due to the expected inclusion of N_2O in the greenhouse gas trade. Besides Fe-zeolites [1-4] and Rh containing catalysts [5, 6], Co-spinels [7-10] seem to be promising catalysts for this reaction at temperatures below 450 °C. Among

them, the Co-Mn-Al mixed oxide with spinel structure (Co:Mn:Al = 4:1:1) prepared by thermal treatment of layered double hydroxide (LDH) precursors was active [11] and stable in the presence of O_2, H_2O and NO_x [12]. Our effort to increase further catalytic activity of the mentioned catalyst led us to the study of the effect of low amounts of promoter incorporation into the catalyst. Alkali promoters, especially potassium, improved catalytic performance dramatically [12, 13]. The intrinsic laboratory data of N_2O catalytic decomposition over K-promoted Co-Mn-Al mixed oxide grains prepared by thermal treatment of LDH was used for model of pilot reactor for abatement of N_2O emissions in off-gases from HNO_3 production. Pseudo-homogeneous one-dimensional model of an ideal plug flow reactor was used for reactor design [14].

In the presented paper, a developed model is being verified, attention will be focused on determination of effective diffusion coefficient and evaluation of mass transfer coefficient effect on N_2O conversion. Pellets of Co-Mn-Al mixed oxide were prepared, tested for N_2O decomposition in an inert gas and the obtained experimental data will be compared with the calculated N_2O conversions based on kinetic data over catalyst grains in kinetic regime. The catalytic reactor for N_2O abatement situated downstream the $DeNO_x$ technology (low NO_x concentration) in nitric acid production unit will be estimated from laboratory data of N_2O decomposition in simulated off gas over Co-Mn-Al mixed oxide pellets.

2. Experimental

The Co-Mn-Al (Co:Mn:Al molar ratio of 4:1:1) mixed oxide catalyst was prepared by calcination (500 °C) of coprecipitated LDH precursor [10]. Five batches were prepared altogether. Four batches were crushed, sieved, marked as Grain-1, Grain-2, Grain-3 and Grain-4 and fraction 0.16 – 0.315 mm was used for the catalytic measurements. The catalysts were characterized in our previous publications [10, 12, 13]. As a fifth batch of the catalyst, we used the pellets (2.7x1.8 mm) prepared by pelletizing of the coprecipitated LDH precursor under such

pressure in order sufficient mechanical strength was achieved (30 MPa). The pellets, calcined 4 h at 500 °C, were marked as Pellets .

The grained catalysts were tested in an integral fixed bed reactor R1. N_2O catalytic decomposition was performed at 300 – 450 °C and 100 – 265 kPa. Inlet gas contained 0.1 molar% N_2O in He and space velocity 20 000 – 60 000 l kg^{-1} h^{-1} was applied.

The catalyst pellets were tested in an integral fixed bed reactor R2. N_2O catalytic decomposition was performed at atmospheric pressure, in temperature range of 240 – 450 °C and space velocity of 6 530 l kg^{-1} h^{-1}. Inlet gas contained 0.1 molar% N_2O in N_2, but gas composition simulating real waste gas from HNO_3 production downstream the $DeNO_x$ (0.1 molar% N_2O, 0.01 molar% NO, 0.01 molar% NO_2, 3 molar% H_2O, 5 molar% O_2) was also applied.

A care was taken to ensure sufficient approach to plug flow conditions in both R1 and R2 reactors. It is supposed that a rectangular velocity profile can be considered [15-17] for ratio:

$$\frac{D_t}{d_p} > 10 \text{ to } 15 \qquad (1)$$

Axial dispersion is negligible [15-17] for:

$$\frac{L_b}{d_p} > \frac{a}{Pe_p} \; ln\left(\frac{1}{1 - X_A}\right), \text{ where } a = 8 \text{ or } 20 \qquad (2)$$

Description of both reactors and verification of validity of conditions (1) and (2) are summarized in Table 1. Both reactors can be considered as isothermal due to the low N_2O concentration leading to maximal adiabatic temperature rise of 4 °C. From the same reason, the absence of internal and external heat transport limitations is supposed [18]. The criterions for 0.95% avoiding the external (3) and internal (4) diffusion limitations [16] were confirmed for all experimental runs in the R1 and R2 reactors.

$$\text{Mears}: \frac{-r_A.\rho_c.r_p.n}{k_c.c_{Ab}} < 0.15 \qquad (3)$$

Weisz-Prater : $$\frac{-r_A \cdot \rho_c . L^2}{D_{eff} \cdot c_{As}} < 0.15 \frac{2}{n+1} \quad (4)$$

3. Mathematical model

Pseudo-homogeneous one-dimensional model of an ideal plug flow reactor in an isothermal regime mentioned in our previous paper [14] was used for modeling of the reactors. The effect of internal and external mass transport was described by overall effectiveness factor Ω, which was incorporated into the 1st order kinetic equation $-r_A = \Omega\, k\, c_A$. In this paper, details of determinations of effective diffusion and mass transfer coefficients are described only.

The effective diffusion coefficient D_{eff} is dependent on morphology of porous catalyst:

$$D_{eff} = \frac{\varepsilon_p}{q} \overline{D} \quad (5)$$

The ε_P/q ratio between 0.05 – 0.1 was published previously [16]. For the determination of the overall diffusivity of N_2O in a multicomponent mixture ($\overline{D}$), the contributions of molecular ($D_{i/j}$) and Knudsen (D_{k,N_2O}) diffusivity was considered together with stoichiometry of the reaction [15]:

$$\frac{1}{\overline{D}} = \frac{1}{D_{k,N_2O}} + \frac{x_{N_2O} + x_{N_2O}}{D_{N_2O/N_2}} + \frac{0.5 \cdot x_{N_2O} + 0.5 \cdot x_{N_2O}}{D_{N_2O/O_2}} + \sum_{j=1}^{n} \frac{x_{N_2O}}{D_{N_2O/j}} \quad (6)$$

where j is component of gas mixture. The Knudsen diffusivity D_{k,N_2O} for pore with radius r_o was determined [16] as:

$$D_{k,N_2O} = 97 \cdot r_o \cdot \sqrt{\frac{T}{M_{N_2O}}} \quad (7)$$

Binary diffusion coefficients $D_{i/j}$ were calculated according to Fuller, Schettler and Giddings [19]:

$$D_{i/j} = \frac{10^{-2} \cdot T^{\frac{7}{4}} \cdot \left(M_j^{-1} + M_i^{-1}\right)^{\frac{1}{2}}}{p \left[\left(\sum v\right)_i^{\frac{1}{3}} + \left(\sum v\right)_j^{\frac{1}{3}}\right]^2} \quad (8)$$

where $\left(\sum v\right)_{N_2} = 17.9$, $\left(\sum v\right)_{N_2O} = 35.9$, $\left(\sum v\right)_{O_2} = 16.6$, $\left(\sum v\right)_{H_2O} = 12.7$,

$\left(\sum v\right)_{He} = 2.88$, $\left(\sum v\right)_{NO} = 11.17$.

Mass transfer coefficient was determined according to correlation of Wakao and Funazkri [20] recommended for fixed bed and 3 < Re < 1000:

$$Sh = 2.0 + (Re)^{1/2}\, 1.1(Sc)^{1/3} \quad (12)$$

4. Results and discussion

Chemical composition and results of analysis of porous structure of the prepared catalysts used in catalytic performance modeling are summarized in Table 2.

4.1 N_2O decomposition over grained Co-Mn-Al mixed oxide catalysts

Temperature dependencies of N_2O conversion over grained Co-Mn-Al mixed oxide catalysts are shown in Fig. 1. The relative error of measured conversions (which includes reproducibility of catalyst preparation and reproducibility of kinetic measurements) increased with decreasing N_2O conversion from 9% to 88%. Kinetic parameters, evaluated according to 1st order rate law by the integral method (Table 2), were used for model verification of the R1 reactor (Table 3). As was required, internal (η) and overall (Ω) effectiveness factors are close to value 1. Only at the highest reaction temperature of 450 °C, the reaction rate is hindered by internal diffusion, whereas at lower temperatures the measurements proceeded in kinetic regime as was confirmed by the values of Mears and Weisz-Prater numbers. Good description of the experimental data was achieved (Fig. 2).

4.2 Influence of pressure on the rate of N_2O catalytic decomposition

Since HNO_3 plants are working at higher pressure, it is important to examine the influence of pressure on the N_2O decomposition rate. The increase of pressure led to the considerably higher N_2O conversions (Fig. 3) due to the increase of N_2O partial pressure and consequent higher reaction rate. The change of pressure can also influence surface species concentrations. When the catalysts surface is covered only slightly, the pressure increase causes higher surface coverage. However, no changes in surface concentrations are observed in the case of saturated surface. The effect of pressure on surface coverage by O_2, NO_x and H_2O will be the subject of our further research.

Higher pressure also lowers binary diffusion coefficients what follows from Eq. (8). The results of the calculated diffusion coefficients in the pressure range of 0.1 – 0.6 MPa are shown in Table 4. Only slight decrease of $D_{i/j}$ was observed in this pressure range, while $\overline{D}$ remained constant and nearly the same as the value of D_{k,N_2O} indicating that Knudsen diffusion is still prevailing in the pores. Further increase of pressure will cause higher gas density leading to the higher frequency of mutual molecule collisions and then, molecule diffusion will become involved, too. Due to decrease in $D_{i/j}$, when the pressure increases, the mass transfer coefficient increased.

4.3 N_2O decomposition over Co-Mn-Al mixed oxide pellets

Effective diffusion coefficient is the most uncertain parameter of the presented model due to the unknown tortuosity and average value of pore size of catalyst particles. Value of ε_p/q in the range of 0.05 – 0.1 is mentioned in literature [16]. In our case D_{eff} determined as $D_{ef} = 0.12\,\overline{D}$ fits the N_2O conversion curves over pellets satisfactory (Fig. 4). Parameters calculated according to the model for N_2O decomposition over catalyst pellets at temperature 450 °C are summarized in Table 3. From Fig. 4 we can see that values of N_2O conversion below 300 °C obtained over

pellets are very close to those obtained for the Grain-2 catalyst in kinetic regime (black dot-and-dash line in Fig. 4). Influence of mass transport limitation appears at higher temperatures i.e. at higher reaction rate. The internal diffusion limitation influences the reaction rate at temperatures higher than 300 °C. According to the value of Mears criterion (Eq. 3), concentration gradients between the bulk gas phase and catalyst surface in the R2 reactor at temperatures higher than 360 °C exist (Table 3). For the purpose of scale-up, the internal diffusion limitation in the pellets can be accounted to kinetic constant, which is considered as microscopic phenomenon. Nearly identical values of the internal and overall effectiveness factor (Table 3) indicate that the reaction rate in R2 reactor is hindered by internal diffusion only. The reason is the order of magnitude higher resistance to the internal mass transfer in comparison with the resistance towards external diffusions. The hindering effect of external mass transport is overlapped by the internal diffusion limitation in the pores of pellets, since the intrusion of the reaction mixture to porous structure is difficult. This is important fact, since we can use the kinetic data obtained over industrial catalyst particles in the R2 laboratory reactor directly for the design of a pilot unit.

Kinetic parameters evaluated according to 1^{st} rate law from the data of N_2O decomposition over pellets in an inert gas and in simulated waste gas are summarized in Table 2, the comparison of calculated and experimental data is shown in Fig. 2. It is evident that 1^{st} order kinetic does not describe the conversions curves precisely. The reason of it can be the complicated temperature dependence of complex kinetic constant, which includes kinetic constant and effectiveness factor. The dependencies of N_2O conversion on space-time for pilot unit designated for abatement of N_2O emission from HNO_3 plant are shown in Fig. 5. For instance, 3 400 kg of Co-Mn-Al mixed oxide pellets (2.7 x 1.8 mm) are necessary for cleaning (90% N_2O conversion) of 30 000 m^3/h (420 °C, 0.6 MPa) leading to the catalyst bed height of 1.7 m in the reactor with diameter of 1.7 m and the pressure drop of 276 kPa.

5. Conclusions

Recently developed pseudo-homogeneous one-dimensional model of a fixed bed reactor was verified with N_2O decomposition over Co-Mn-Al mixed oxide catalysts grains and pellets. Higher working pressure had positive impact on the N_2O decomposition rate. Therefore, the suitable position of N_2O decomposition reactor in HNO_3 plant is upstream the expansional turbine. Kinetic data measured over the catalyst pellets and described by 1st order rate law can be directly used for estimation of the catalytic unit for N_2O abatement in HNO_3 plant.

Acknowledgements

This work was supported by the Technology Agency of the Czech Republic (project No. TA 01020336) and EU project No. CZ.1.05/2.1.00/03.0100 „Institute of Environmental Technologies“.

Nomenclature

c_A	Concentration of A	(mol m^{-3})
c_{Ab}	Concentration of A in bulk of gas	(mol m^{-3})
c_{As}	Concentration of A on the catalyst surface	(mol m^{-3})
d_p	Catalyst particle diameter	(m)
$\overline{D}$	Overall diffusivity	(m^2 s^{-1})
D_a	Axial dispersion coefficient	(m^2 s^{-1})
D_{eff}	Effective diffusion coefficient	(m^2 s^{-1})
$D_{i/j}$	Binary diffusion coefficient of molecular diffusivity	(m^2 s^{-1})
D_{k,N_2O}	Knudsen diffusivity	(m^2 s^{-1})
D_t	Reactor tube diameter	(m)
E_a	Activation energy	(J mol^{-1})
k	Kinetic constant, 1st order rate law	(m^3 s^{-1} kg^{-1})
k_c	Mass transfer coefficient	(m s^{-1})
k_o	Pre-exponential factor	(m^3 s^{-1} kg^{-1})
L	Characteristic dimension of catalyst particle	(m)
L_b	Length of catalyst bed	(m)
M_i	Molar weight of *i* compound	(g mol^{-1})
n	Reaction order	(-)

199	p	Pressure	(Pa)
200	Δp	Pressure drop	(Pa)
201	$Pe_p = \frac{v.d_p}{D_a}$	Peclet number	(-)
202	q	Tortuosity	(-)
203	$-r_A$	Reaction rate of component *A*	(mol s^{-1} g^{-1})
204	r_o	Catalyst pore radius	(m)
205	r_p	Catalyst particle radius	(m)
206	$Re = \frac{v.d_p.\rho}{\eta_g}$	Reynolds number	(-)
207	S_{BET}	Specific surface area	(m^2g^{-1})
208	$Sc = \frac{\eta_g}{\rho.D_{N2O/j}}$	Schmidt number, *j* is carrier gas	(-)
209	$Sh = \frac{k_c d_p}{D_{N2O/j}}$	Sherwood number, *j* is carrier gas	(-)
210	T	Thermodynamic temperature	(K)
211	v	Superficial velocity	(m s^{-1})
212	w	Weight of catalyst	(kg)
213	x_{N_2O}	Molar fraction of N_2O	(-)
214	X_A	Conversion of component A	(-)
215			
216	Greek letters		
217	ε_p	Porosity of catalyst particle	(-)
218	η	Internal effectiveness factor	(-)
219	η_g	Dynamic viscosity	(Pa s)
220	ρ	Density of gas	(kg m^{-3})
221	ρ_c	Bulk density of catalyst	(kg m^{-3})
222	Ω	Overall effectiveness factor	(-)
223	(Σv)	Diffusion volume	(-)

224

225 **References**

226 [1] S. Sklenak, P. C. Andrikopoulos, B. Boekfa, B. Jansang, J. Nováková, L. Benco, T.
227 Bucko, J. Hafner, J. Dědeček, Z. Sobalík, J.Catal. 272 (2010) 262-274.

[2] N. Liu, B. Chen, Y. Li, R. Zhang, X. Liang, Y. Li, Z. Lei, J. Phys. Chem. C 115 (2011) 12883-12890.

[3] M.-Y. Kim, K. W. Lee, J.-H. Park, C.-H. Shin, J. Lee, G. Seo, Korean J. Chem. Eng. 27 (2010) 76-82.

[4] H. Guesmi, D. Berthomieu, L. Kiwi-Minsker, J. Phys. Chem. C 112 (2008) 20319-20328.

[5] H. Beyer, J. Emmerich, K. Chatziapostolou, K. Köhler, Appl. Catal. A 391 (2011) 411-416.

[6] J. Haber, M. Nattich, T. Machej, Appl. Catal. B 77 (2008) 278-283.

[7] M. Inger, P. Kowalik, M. Saramok, M. Wilk, P. Stelmachowski, G. Maniak, P. Granger, A. Kotarba, Z. Sojka, Catal Today 176 (2011) 365-368.

[8] H. Cheng, Y. Huang, A. Wang, L. Li, X. Wang, T. Zhang, Appl. Catal. B 89 (2009) 391-397.

[9] K. Asano, C. Ohnishi, S. Iwamoto, Y. Shioya, M. Inoue, Appl. Catal. B 78 (2008) 242-249.

[10] L. Obalová, K. Jirátová, F. Kovanda, K. Pacultová, Z. Lacný, Z. Mikulová, Appl. Catal. B 60 (2005) 297-305.

[11] L. Obalová, K. Pacultová, J. Balabánová, K. Jirátová, Z. Bastl, M. Valášková, Z. Lacný, F. Kovanda, Catal. Today 119 (2007) 233-238.

[12] L. Obalová, K. Karásková, K. Jirátová, F. Kovanda, Appl. Catal. B 90 (2009) 132-140.

[13] K. Karásková, L. Obalová, K. Jirátová, F. Kovanda, Chem. Eng. J. 160 (2010) 480-487.

[14] L. Obalová, K. Jirátová, K. Karásková, F. Kovanda, Chin. J. Catal. 32 (2011) 816-820.

[15] M. Kraus, P. Schneider, L. Beránek, Chemická kinetika pro inženýry, SNTL, Praha, 1978.

[16] F. Kaptejn, J. A. Moulijn, in: G. Ertl, H. Knözinger, J. Weitkamp, Handbook of Heterogeneous Catalysis, Vol. 3, Wiley, Weinheim, 1996.

[17] H. S. Fogler, Elements of Chemical Reaction Engineering, third ed., Prentice Hall PTR, New Jersey, 1999.

[18] K. Galejová, L. Obalová, K. Jirátová, K. Pacultová, F. Kovanda, Chem. Pap. 63 (2009) 172-179.

[19] E. N. Fuller, P. D. Schettler, J. C. Giddings, Ind. Eng. Chem. 58 (1966) 19-24.

262 [20] N. Wakao, T. Funazkri, Chem. Eng. Sci. 33 (1978) 1375-1384.

263

Table 1 Description of experimental reactors R1 and R2

Reactor	D_t (mm)	Catalyst weight w (g)	Catalyst size (mm)		Length of bed [1] L_b (mm)	D_t/d_p [2]	L_b/d_p [2]
R1	5	0.1000	spheres	0.160-0.315	20	16	63 (required minimal value 15-38)[3]
R2	40	4.5940	pellets	2.7 x 1.8	150	15	55 (required minimal value 48-120)[3]

[1] Including inert particles with approximately same diameter, [2] The biggest particles are considered for verification of plug flow, [3] Calculated for 95% N_2O conversion and Pe_p = 0.5 valid for low Re [15]

Table 2 Chemical composition, porous structure and kinetic parameters determined for 1st order rate law from experiments of N_2O decomposition

Catalyst	Molar ratio Co:Mn:Al	S_{BET} ($m^2\ g^{-1}$)	r_0 (nm)	ρ_c [3] ($kg\ m^{-3}$)	E_a ($J\ mol^{-1}$)	ln k_0 ($m^3\ s^{-1}\ g^{-1}$)
Grain-1	4 : 1.15 : 1.57	93	12.0[1]	880	114 908[4]	9.76[4]
Grain-2	4 : 1.39 : 1.58	98	n.d.[6]	n.d.[6]	106 985[4]	8.31[4]
Grain-3	4 : 1.29 : 1.56	92	n.d.[6]	n.d.[6]	97 290[4]	6.75[4]
Grain-4	4 : 1.05 : 1.05	93	12.0[1]	n.d.[6]	109 421[4]	9.38[4]
Pellets	n.d.[6]	115	14.8[2]	1 282	75 799[4] 116 521[5]	1.96[4] 7.53[5]

[1] Average pore radius determined from desorption branch of N_2 adsorption isotherm, [2] Average pore radius determined from Hg porozimetry, [3] Bulk density determined from Hg porozimetry, [4] Inert gas, [5] Waste gas, [6] Not determined.

Table 3 Parameters calculated for N_2O decomposition over catalyst Grain-1 and Pellets

Conditions: 0.1 molar% N_2O in He (Grain-1) or in N_2 (Pellets) in laboratory reactor R1 and R2, respectively, temperature 450 °C, 0.1 MPa

Catalyst	GHSV ($l\ h^{-1}\ kg^{-1}$)	v (m/s)	Re (-)	$\overline{D}$ (m^2/s)	$D_{N_2O/j}$ [1] (m^2/s)	D_{eff} (m^2/s)	D_{k,N_2O} (m^2/s)	k_c (m/s)	η (-)	Ω (-)	Mears (-)	Weisz-Prater (-)	Δp (Pa)
Grain-1 [2]	60 000	0.22	0.1	$4.72 \cdot 10^{-6}$	$2.36 \cdot 10^{-4}$	$4.72 \cdot 10^{-7}$ [3]	$4.72 \cdot 10^{-6}$	2.35	0.92	0.92	0.003	0.252	4750
Pellets	6 530	0.02	0.7	$5.80 \cdot 10^{-6}$	$6.98 \cdot 10^{-5}$	$6.96 \cdot 10^{-7}$ [4]	$5.80 \cdot 10^{-6}$	0.07	0.22	0.21	0.874	28	280

[1] j = He for grains, j = N_2 for pellets, [2] Average grain size, [3] $D_{eff} = 0.1\,\overline{D}$, [4] $D_{eff} = 0.12\,\overline{D}$

Table 4 Influence of pressure on diffusion coefficients and mass transfer coefficient

Conditions: 0.1 molar% N_2O in He, GHSV = 60 000 l h^{-1} kg^{-1}, Grain-1, 360 °C

Pressure (MPa)	$D_{N_2O/He}$ (m^2/s)	D_{N_2O/O_2} (m^2/s)	D_{N_2O/N_2} (m^2/s)	D_{k,N_2O} (m^2/s)	$\overline{D}$ (m^2/s)	D_{eff} [1] (m^2/s)	k_c (m/s)
0.1	$1.87 \cdot 10^{-4}$	$5.43 \cdot 10^{-5}$	$5.53 \cdot 10^{-5}$	$4.42 \cdot 10^{-6}$	$4.41 \cdot 10^{-6}$	$4.41 \cdot 10^{-7}$	0.19
0.6	$3.18 \cdot 10^{-5}$	$9.24 \cdot 10^{-6}$	$9.40 \cdot 10^{-6}$	$4.42 \cdot 10^{-6}$	$4.41 \cdot 10^{-6}$	$4.41 \cdot 10^{-7}$	0.32

[1] D_{eff} calculated as $D_{eff} = 0.1\,\overline{D}$

Figure captions

Fig. 1 Temperature dependence of N_2O conversion over grained Co-Mn-Al mixed oxide catalysts at GHSV = 60 000 l kg^{-1} h^{-1} and atmospheric pressure.

Fig. 2 Comparison of measured N_2O conversions and conversion calculated according to 1st order kinetic equation evaluated from experimental data measured over grains (e.g. in kinetic regime) and over the pellets (e.g. including internal diffusion).

Fig. 3 Dependence of N_2O conversion on pressure over Grain-1catalyst.
Conditions: 360°C, GHSV = 60 000 l kg^{-1} h^{-1}, 0.1 molar% N_2O in He.

Fig. 4 Dependence of N_2O conversion over the pellets on the effective diffusion coefficient at temperatures 240 – 450 °C.
Conditions: GHSV = 6 530 l kg^{-1} h^{-1}, 0.1 molar% N_2O in N_2, 0.1 MPa, kinetic parameters obtained over Grain-2 and $-r_A = \Omega\, k\, c_A$ was used for N_2O decomposition modeling.

Fig. 5 Dependence of calculated N_2O conversion on space time in pilot reactor for N_2O decomposition in waste gas from HNO_3 plant.
Conditions: inlet pressure 0.6 MPa, D_t =1.7 m, v = 0.62 m s^{-1}, kinetic equation $-r_A = exp\left(\frac{-116521}{RT} + 7.53\right)$.

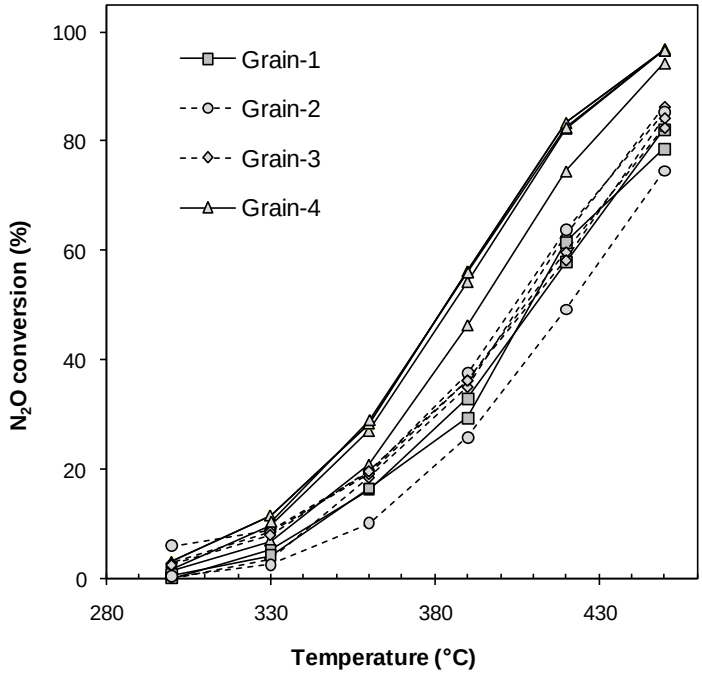

308

309 **Fig. 1**

310

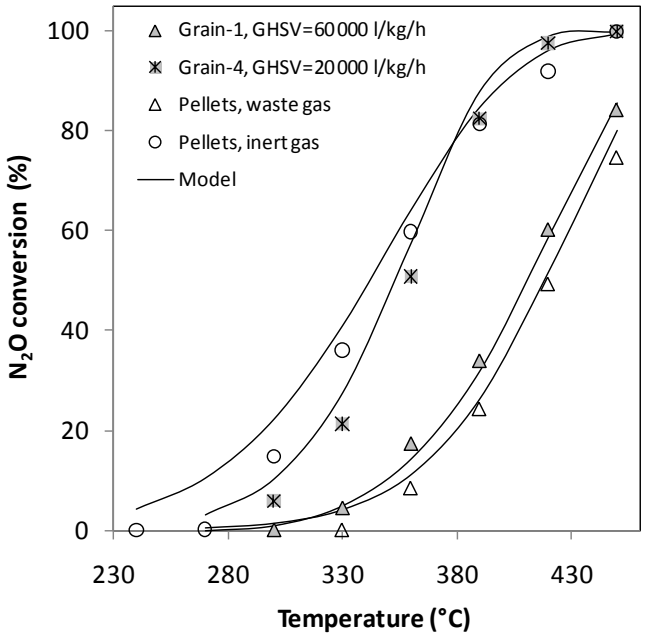

311

312 **Fig. 2**

313

314

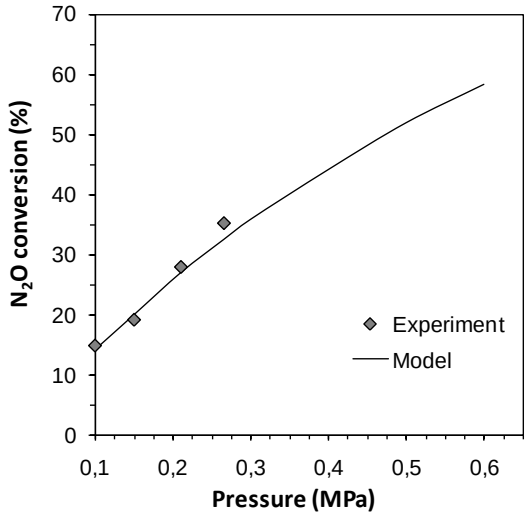

315

316 **Fig. 3**

317

318

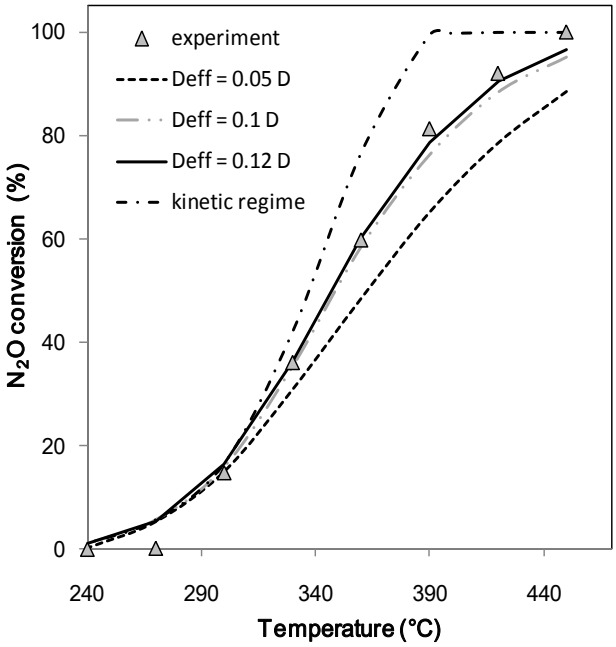

319

320

321 **Fig. 4**

322

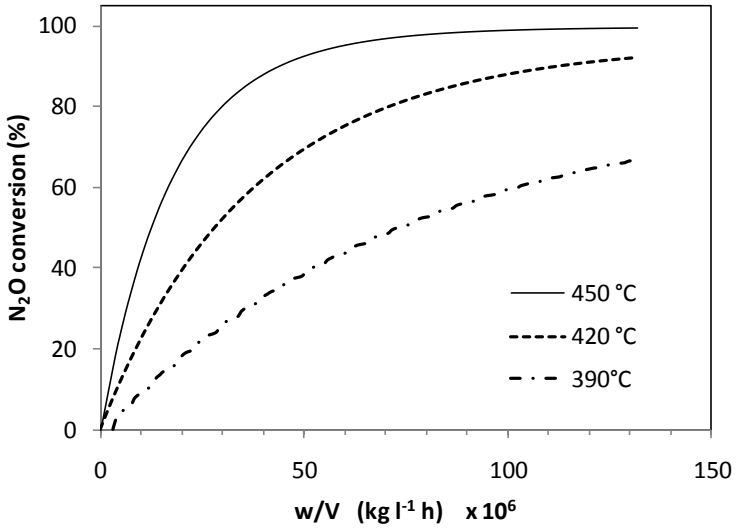

Fig. 5